I.J. Wireless and Microwave Technologies, **2026, 3, 128-141**
Published Online on June 8, 2026 by MECS Press (http://www.mecs-press.org/)
DOI: 10.5815/ijwmt.2026.03.09

A Physics-Informed Heterogeneous Graph Transformer Model for Managing Heterogeneous Big Data in Urban Construction Projects

Olga Solovei*
Dept. of Information Technologies of the Kyiv National University of Construction and Architecture, Kyiv, 03037, Ukraine
E-mail: solovey.ol@knuba.edu.ua
ORCID iD: https://orcid.org/0000-0001-8774-7243
*Corresponding Author

Tetiana Honcharenko
Dept. of Information Technologies of the Kyiv National University of Construction and Architecture, Kyiv, 03037, Ukraine
E-mail: goncharenko.ta@knuba.edu.ua
ORCID iD: https://orcid.org/0000-0003-2577-6916

Received: 20 March, 2026; Revised: 20 April, 2026; Accepted: 28 May, 2026; Published: 28 June, 2026

Abstract: This research aims to enhance predictive maintenance and inspection planning in urban construction projects. Recent advances in graph neural networks and graph transformer architecture have demonstrated significant potential for modeling complex lifecycle processes of building systems. However, most existing approaches remain predominantly data-driven and lack integration of physics-informed modeling and real-time data, which limits their applicability in large-scale urban environments. This research addresses this gap by proposing an approach for managing heterogeneous big data in urban construction projects, enabling prediction of the technical condition and inspection needs of structural elements. The core contribution is the development of a physics-informed heterogeneous graph transformer model that integrates domain-specific physical knowledge into the learning process through physics-based features and regularization mechanisms. The results confirm that all validation criteria are simultaneously satisfied: the difference between training and validation accuracy remains within the threshold (ϵ=0.05); The overall classification accuracy exceeds 92.06%; area under ROC curve above 0.8; F1-score is above 0.8 for all major classes; Physics-alignment error is lower than 0.15; and a strong Spearman correlation is observed between model predictions and physics-based indicators. The novelty of the proposed approach lies in the development of a physics-informed graph learning paradigm which enables the integration of structural mechanics, degradation processes, and heterogeneous data sources within a unified predictive framework.

Index Terms: Physics-informed learning, heterogeneous graph transformer, graph neural network, predictive maintenance, building information modeling

1. Introduction

The increasing complexity of construction projects led to the generation of heterogeneous data across all phases of the building lifecycle, including design, construction, and operation [1].

These data originate from multiple sources, such as Building Information Modeling (BIM) systems, Internet of Things (IoT) sensors, inspection records, and environmental monitoring platforms. Effective management and analysis of such heterogeneous big data are critical for sustainable urban development [2].

Recent advances in graph neural networks (GNNs) and graph transformers have demonstrated potential in modeling complex relational data structures. In particular, heterogeneous graph neural networks enable the representation of BIM data as multi-typed graphs, where nodes correspond to building components and spatial entities, and edges encode structural, functional, and spatial relationships. Such approaches allow capturing high-order dependencies and contextual interactions within building systems. Despite these advancements, existing approaches remain limited in several critical aspects. Most models are purely data-driven and do not incorporate physics-based

This work is open access and licensed under the Creative Commons CC BY 4.0 License.

knowledge, such as structural mechanics, material degradation processes, and environmental impact. BIM and IoT data streams are treated in isolation which does not allow to capture real-time impacts on BIM model.

To address these limitations, this research proposes a new framework to integrate: heterogeneous graph transformer architecture for modeling complex relational structures of BIM data; physics-informed features and constraints, derived from structural and environmental models for enhancing interpretability and reliability.

2. Research Goal and Objectives

The research goal is to develop a physics-informed heterogeneous graph-based approach as a core component of a hybrid information technology for managing heterogeneous big data in urban construction projects, enabling prediction of the technical condition and inspection needs of structural elements.

To achieve this goal, the following research objectives are defined:

To develop a physics-informed heterogeneous graph transformer (HGT) model that integrates domain-specific physical knowledge into the graph neural network architecture through physics-based features and regularization mechanisms.

To develop a training and validation methodology for the proposed model, including multi-criteria evaluation of predictive performance, generalization ability, and physical consistency.

To experimentally validate the proposed approach on synthetic datasets generated from IFC-based BIM models.

3. Related Work

Research [3] proposes a BIM-based heterogeneous graph neural network (HGNN) framework for spatial semantic reasoning and lifecycle management. In this approach, IFC-based BIM data are transformed into a heterogeneous graph consisting of: space (rooms, zones) and components (walls, slabs, HVAC elements) node types; space–space, space–component, and component–component relations edge types. The model employs an HGTConv-based architecture with: type-specific projections; relation-aware message passing; multi-head attention; meta-path-based reasoning. This allows capturing high-order dependencies between spatial and functional building elements. The approach successfully demonstrates the applicability of heterogeneous graph transformers for anomaly detection and lifecycle reasoning. However, the framework remains purely data-driven, lacking: physics-informed modeling; real-time data integration which limits its applicability in safety-critical and large-scale urban systems.

Another direction is the development of pretrained graph neural networks for BIM representation learning is proposed in [4]. The BIGNet model, which converts BIM into heterogeneous graphs with: semantic nodes (building elements); topological nodes (relationships); spatial nodes (proximity-based relations). The model is pretrained using a self-supervised masked autoencoder strategy, enabling learning from large unlabeled BIM datasets. The learned embeddings are then transferred to downstream tasks such as: semantic conflict detection; topology validation; design error identification. This approach significantly improves data efficiency and generalization. However, BIGNet operates on static BIM snapshots and relies only on: geometric, semantic, and relational features. It does not incorporate physics-based degradation indicators, limiting its ability to model the actual physical state of structures.

A group of studies focuses on context-aware learning for BIM element classification and quality validation. In [5] a property graph is constructed where: nodes represent BIM elements; edges represent spatial proximity. The study compares classical ML methods (Logistic Regression, Random Forest, SVM) with GNN models (GCN, GraphSAGE, TransformerConv), demonstrating that: incorporating relational context significantly improves classification accuracy. In research [6] further extend this idea by introducing ContextNet, which uses a dual-encoder architecture: one encoder for the target element geometry; one encoder for surrounding context geometry. This allows capturing local geometric context, improving classification performance. Despite these advances, both approaches are limited by: reliance on local context only; absence of global relational reasoning; lack of temporal and physics-based modeling. Thus, they remain insufficient for complex lifecycle and reliability analysis tasks.

Research [7] proposes a Transformer-based framework for energy consumption prediction, integrating: BIM data (geometry, materials, semantics); IoT sensor streams (HVAC, environment, occupancy). The system is structured into four layers: data acquisition; BIM integration; Transformer-based intelligence layer; application layer. The model demonstrates strong performance due to: multi-modal data fusion; attention-based temporal modeling; incorporation of BIM as a domain prior. However, the approach: does not use graph-based representations; focused only on energy prediction, not structural safety. Thus, it cannot support comprehensive lifecycle management of building systems.

Recent advancements in graph transformers aim to improve representation learning through architectural innovations. Work [8] introduces a graph transformer with heterogeneous memory, where: memory stores historical node representations; attention mechanisms incorporate long-range dependencies; heterogeneous semantic patterns are preserved. This improves representation stability, performance on sparse data, and long-range dependency modeling. However, this approach is designed for recommendation systems, lacks engineering interpretability. Therefore, it is not directly applicable to construction and infrastructure systems, where physical consistency and safety are critical.

Based on the reviewed studies, four major research directions are identified: Graph-based BIM modeling, Context-

aware BIM analysis, Multi-modal BIM–IoT integration, Advanced graph transformer architectures.

None of the reviewed approaches integrate structural mechanics, degradation processes, reliability theory.

Thus, they cannot ensure physically consistent predictions. These limitations justify the need for a hybrid, physics-informed heterogeneous graph transformer framework, capable of supporting structural reliability assessment in urban construction systems.

4. Methodology

4.1. Architecture of physics-informed heterogeneous graph transformer model

Let a heterogeneous graph be defined as:

$$G = (V, E, X) \tag{1}$$

Where:

- V is the set of nodes, E is the set of edges, and X denotes node features.
- $\forall u \in V$ is assigned a node type $\tau(u) \in T$.
- $\forall v \in V$ is assigned a node type $\tau(v) \in T$ and $\forall e_{uv} \in E$ (from source node u to target node v) has a relation type $\phi(e_{uv}) \in R$.

T is a set of node types derived from IFC element categories; R is a set of edge types which are supported in graph G.

For each node v, the feature vector $x_v \in R^{d_{in}}$ is composed of three groups of features: geometric characteristics x^{geom}, degradation-related parameters x^{deg}; a scalar physics-informed indicator $x_{physics}$:

$$x_v = \left[x_v^{geom}, x_v^{deg}, x_{physics,v}\right] \tag{2}$$

The geometric component encodes spatial and topological properties extracted from the BIM model, while x_v^{geom} represents time-dependent degradation processes obtained from physics-based models. The scalar feature $x_{physics,v}$ is derived from a structured set of physics-informed variables defined for each structural element type $m \in$ {column, beam, slab, wall} as a pair:

$$\left(x_{physics}^{(m)}, v^{(m)}\right) \tag{3}$$

Where:

- $x_{physics}^{(m)}$ denotes a vector of continuous normalized physical indicators.
- $v^{(m)}$ is a vector of binary violation indicators used in inspection decision I_m.

Formal definition of vectors $x_{physics}^{(m)}$ and $v^{(m)}$ is given in paper [9].

For reinforced concrete columns, the physics feature vector and violation vectors are defined as:

$$x_{physics}^{(C)} = \left[\frac{2.5}{SF_{col}}, \frac{r_{loss}}{c_{cover}}, i_{corr}\right]^T \tag{4}$$

$$v^{(C)} = [\mathbb{I}(SF_{col} < 5.5), \mathbb{I}(r_{loss} > 0.3c_{cover})]^T \tag{5}$$

Where:

- SF_{col} is the safety factor of the column.
- r_{loss} is the time-dependent loss of rebar radius.
- i_{corr} is the corrosion current density; c_{cover} is the concrete cover thickness.

The inspection indicator is defined as $I_C = \mathbb{I}\left(v_1^{(C)} \vee v_2^{(C)}\right)$.

For beams, the physics feature vector and violation vectors are defined as:

$$x_{physics}^{(b)} = \left[\frac{2.0}{SF_{beam}}, \frac{a_{final}}{0.012}, \frac{K_I}{0.85K_{IC}}, \frac{\sigma_s/\sigma_y}{0.8}, \frac{a_{final}/a_0}{3.0}\right]^T \tag{6}$$

$$\mathrm{v}^{(\mathrm{b})} = \begin{bmatrix} \mathbb{I}(\mathrm{a_{final}} > 0.012), \mathbb{I}(\mathrm{SF_{beam}} < 2.0), \mathbb{I}(\mathrm{K_I} \geq 0.85\mathrm{K_{IC}}), \mathbb{I}\left(\sigma_\mathrm{s}/\sigma_\mathrm{y} > 0.8\right), \\ \mathbb{I}(\mathrm{a_{final}}/\mathrm{a_0} > 3.0) \end{bmatrix}^{\mathrm{T}} \quad (7)$$

Where:

- a_0, a_{final} are initial and final cracks length.
- K_I - the stress intensity factor; K_{IC} is the fracture toughness of the material.
- σ_s is the bending stress; σ_y is the yield strength.

The inspection indicator is defined as $I_B = \mathbb{I}\left(\mathrm{V}_{i=1}^{5}\, \mathrm{v}_i^{(b)}\right)$.

For slabs, the physics feature vector and violation vectors are defined as:

$$\mathrm{x}_{\mathrm{physics}}^{(\mathrm{s})} = \left[\frac{\sigma_{\mathrm{slab}}}{0.9\sigma_\mathrm{y}}, \frac{\mathrm{WLI}}{0.5}, \frac{\mathrm{w_{crack}}}{0.3}, \frac{\mathrm{d_{corr}}}{0.7\mathrm{c_{cover}}}, \frac{\triangle \mathrm{S}}{25}\right]^{\mathrm{T}} \quad (8)$$

$$\mathrm{v}^{(\mathrm{s})} = \left[\mathbb{I}\left(\sigma_{\mathrm{slab}} > 0.9\sigma_\mathrm{y}\right), \mathbb{I}(\mathrm{WLI} > 0.5), \mathbb{I}(\mathrm{w_{crack}} > 0.3), \mathbb{I}(\mathrm{d_{corr}} > 0.7\mathrm{c_{cover}}), \mathbb{I}(\triangle \mathrm{S} > 25)\right]^{\mathrm{T}} \quad (9)$$

Where σ_{slab} is the stress in reinforcement; WLI is water leakage index; w_{crack} is the crack width; σ_y is the nominal yield strength of the steel reinforcement; WLI_{crit} is the critical threshold value for the water leakage index ; d_{corr} is corrosion penetration depth; c_{cover} is the thickness of the concrete cover; ΔS is the settlement-induced deformation.

The inspection indicator is defined as $I_S = \mathbb{I}\left(\mathrm{V}_{i=1}^{5}\, \mathrm{v}_i^{(s)}\right)$.

For wall, the physics feature vector and violation vectors are defined as:

$$\mathrm{x}_{\mathrm{physics}}^{(\mathrm{w})} = \left[\frac{Eff_{loss}}{18.0}, \frac{\mathrm{MI}}{5.5}, \frac{10 - \mathrm{C_{sealant}}}{0.8}, \frac{\mathrm{U_{maint}}}{0.7}\right]^{\mathrm{T}} \quad (10)$$

Server keeps a hash (or quantum finger prints) for future verification:

$$\mathrm{v}^{(\mathrm{w})} = [\mathbb{I}(0 < \mathrm{Y_{fail}} < 1), \mathbb{I}(Eff_{loss} > 25), \mathbb{I}(\mathrm{MI} > 7), \mathbb{I}(\mathrm{U_{maint}} > 8.5)]^{\mathrm{T}} \quad (11)$$

Where Eff_{loss} is the loss of energy efficiency; MI is the moisture index; $C_{sealant}$ is the sealant condition index; U_{maint} is the maintenance urgency index; Y_{fail} is the predicted time to failure.

The inspection indicator is defined as $I_W = \mathbb{I}\left(\mathrm{V}_{i=1}^{4}\, \mathrm{v}_i^{(w)}\right)$.

The scalar physics-informed indicator incorporated into the node feature vector is defined as:

$$\mathrm{x}_{\mathrm{physics},\upsilon} = \mathrm{clamp}_{[0,1]}\left(\alpha_\mathrm{m}\mathrm{s}_{\mathrm{physics}}^{(\mathrm{m})} + \beta \mathrm{I}_\mathrm{m}\right) \quad (12)$$

Where $clamp_{[0,1]} = min(1, max(0, x)$ is the normalization function; α, β controls the contribution of each term.

The following parameters in $x_{physics}$ are obtained IoT-based simulation streams: Relative humidity RH, Temperature T, Chloride concentration C_{cl}, Precipitation P_{precip}, UV exposure T_{UV}.

The initial node embedding is obtained via a type-specific projection:

$$\mathrm{h}_\upsilon^{(0)} = \mathrm{ReLU}\left(\mathrm{W}_{\tau(\upsilon)}\mathrm{x}_\upsilon\right) \quad (13)$$

Where:

- $W_{\tau(v)} \in R^{d \times din}$ is a learnable matrix for node type τ(v).
- d is the hidden dimension.

For each attention head k∈{1,…,H}, the model learns [10]:

$$\{\mathrm{W}_\mathrm{Q}^{\tau,\mathrm{k}}, \mathrm{W}_\mathrm{K}^{\tau,\mathrm{k}}, \mathrm{W}_\mathrm{V}^{\tau,\mathrm{k}}, \mathrm{W}_\mathrm{R}^{\phi,\mathrm{k}}, \mathrm{W}_\mathrm{M}^{\phi,\mathrm{k}}\} \quad (14)$$

Where:

- $W_Q^{\tau,k}, W_K^{\tau,k}, W_V^{\tau,k}$ are independent learnable weight matrices for each attention head k.
- $W_R^{\phi,k}$ is a relation-type-specific transformation used in attention; $W_M^{\phi,k}$ is a relation-type-specific message transformation.

At layer ℓ, for a target node v and source node $u \in \mathcal{N}(v)$ the query (q), key (k), and value (v) vectors are defined as [11]:

$$\mathrm{q}_{\mathrm{v}}^{(\mathrm{k})} = \mathrm{W}_{\mathrm{Q}}^{\tau(\mathrm{v}),\mathrm{k}} \mathrm{h}_{\mathrm{v}}^{(\ell)}, \mathrm{k}_{\mathrm{u}}^{(\mathrm{k})} = \mathrm{W}_{\mathrm{K}}^{\tau(\mathrm{u}),\mathrm{k}} \mathrm{h}_{\mathrm{u}}^{(\ell)}, \mathrm{v}_{\mathrm{u}}^{(\mathrm{k})} = \mathrm{W}_{\mathrm{V}}^{\tau(\mathrm{u}),\mathrm{k}} \mathrm{h}_{\mathrm{u}}^{(\ell)} \tag{15}$$

The unnormalized attention score between node u and node v is computed as [12]:

$$e_{uv}^{(k)} = \frac{\left(q_v^{(k)}\right)^T W_R^{\phi(e_{uv}),k} k_u^{(k)}}{\sqrt{d_k}} \tag{16}$$

Where $d_k = d/H$ is the dimensionality of each attention head.
The normalized attention coefficient is:

$$\alpha_{uv}^{(k)} = \frac{exp\left(e_{uv}^{(k)}\right)}{\sum_{z \in \mathcal{N}(v)} exp\left(e_{zv}^{(k)}\right)} \tag{17}$$

The message passed from node u to node v under attention head k is:

$$m_{uv}^{(k)} = \alpha_{uv}^{(k)} W_M^{\phi(e_{uv}),k} v_u^{(k)} \tag{18}$$

Messages are aggregated across neighbors and attention heads as:

$$\tilde{h}_v^{(\ell+1)} = \Big\|_{k=1}^{H} \left(\sum_{u \in \mathcal{N}(v)} m_{uv}^{(k)} \right) \tag{19}$$

Where || denotes concatenation across heads.
The updated node representation is computed as:

$$h_v^{(\ell+1)} = Dropout\left(ReLU\left(W_O^{\tau(v)} \tilde{h}_v^{(\ell+1)} + h_v^{(\ell)}\right)\right) \tag{20}$$

Where $W_O^{\tau(v)}$is a learnable matrix that combines information from all attention heads for node type τ(v); the residual connection $+h_v^{(\ell)}$ to improve training stability.

After L layers, the predicted class probabilities for node v are computed as:

$$\hat{y}_v = softmax\left(W_{cls}^{\tau(v)} h_v^{(L)}\right) \tag{21}$$

Where $W_{cls}^{\tau(v)}$ is final classification weight matrix.
The total loss function is defined as:

$$\mathcal{L} = \mathcal{L}_{CE} + \lambda \mathcal{L}_{physics} \tag{22}$$

Where $\mathcal{L}_{CE} = -\sum_{v \in V} y_v \, log \hat{y}_v$ is a cross-entropy loss; $\mathcal{L}_{physics} = \frac{1}{|V|} \sum_{v \in V} \left(\hat{y}_{v,1} - x_{physics,v}\right)^2$ is a physics-based regularization; $\hat{y}_{v,1}$ denoting the predicted probability of the positive class; λ controls the contribution of the physics term.

4.2. Methodology to train a physics-informed heterogeneous graph transformer model

The methodology for training of the physics-informed HGT is described by pseudo code in Algorithm 1. The algorithm consists of blocks: 1) forward propagation; 2) prediction and criticality evaluation; 3) loss computation; 4) backpropagation with parameter update. During each training epoch, node embeddings are first computed as $h_u^{(0)} = ReLU(W_{\tau(u)} x_u)$. For each layer ℓ, messages are propagated from neighboring nodes using the attention mechanism defined in Section 4.1, producing updated embeddings $h_v^{(\ell+1)}$. After the forward propagation, predictions are computed as $\hat{y}_u = softmax\left(W_{cls}^{\tau(u)} h_u^{(L)}\right)$. The entropy-based uncertainty is calculated as [13]:

$$U_u = -\sum_c \hat{y}_{u,c} \, log \hat{y}_{u,c} \tag{23}$$

The critical score is defined as:

$$\text{critical_score}_u = \alpha \cdot x_{physics,u} + \beta \hat{y}_{u,1} + \gamma U_u \tag{24}$$

The total loss $\mathcal{L}$ is computed as defined in Section 4.1. Model parameters are updated using gradient descent as [14]:

$$\nabla_\theta \mathcal{L} \longleftarrow \frac{\partial \mathcal{L}}{\partial \theta}, \theta \leftarrow \theta - \eta \nabla_\theta \mathcal{L} \tag{25}$$

Where η is the learning rate.

The procedure is repeated until either: there is no increase in validation loss for 5 consecutive epochs, or the number of epochs reached maximum N_{epoch}.

Algorithm 1. Training procedure of the physics-informed HGT

Input: heterogeneous graph G=(V,E,X), node types T, edge types R, labels y_u for u∈V, number of attention heads H, number of layers L, physics-loss weight λ, number of epochs N_{epoch}.

Output: trained parameters θ, predicted probabilities $\hat{y}_u$, critical score critical_score_u for all $u \in V$

Initialize: model parameters $\theta = \{W_Q^{\tau,k}, W_K^{\tau,k}, W_V^{\tau,k}, W_R^{\phi,k}, W_M^{\phi,k}\}$ randomly; current epoch n= 0;

repeat

1.Forward propagation

for each node u ∈ V do

$h_u^{(0)} = ReLU(W_{\tau(u)} x_u)$,

endfor

for ℓ =1 to L-1 do

for each target node $v \in V$do

Initialize $\tilde{h}_v^{(\ell+1)} \leftarrow \emptyset$

for k =1 to H do

for each source node u ∈ N(v) do

$q_v^{(k)} = W_Q^{\tau(v),k} h_v^{(\ell)}$, $k_u^{(k)} = W_K^{\tau(u),k} h_u^{(\ell)}$, $v_u^{(k)} = W_V^{\tau(u),k} h_u^{(\ell)}$.

$e_{uv}^{(k)} = \frac{\left(q_v^{(k)}\right)^T W_R^{\phi(e_{uv}),k} k_u^{(k)}}{\sqrt{d_k}}$

endfor

for each source node u∈ N(v) do

$\alpha_{uv}^{(k)} = \frac{exp\left(e_{uv}^{(k)}\right)}{\sum_{z \in \mathcal{N}(v)} exp\left(e_{zv}^{(k)}\right)}$

$m_{uv}^{(k)} = \alpha_{uv}^{(k)} W_M^{\phi(e_{uv}),k} v_u^{(k)}$

endfor

$z_v^{(k)} \longleftarrow \sum_{u \in \mathcal{N}(v)} m_{uv}^{(k)}$

$\tilde{h}_v^{(\ell+1)} = \tilde{h}_v^{(\ell+1)} || z_v^{(k)}$

endfor

$h_v^{(\ell+1)} = Dropout\left(ReLU\left(W_O^{\tau(v)} \tilde{h}_v^{(\ell+1)} + h_v^{(\ell)}\right)\right)$

endfor

endfor

2. Prediction and criticality evaluation

for each node u∈Vdo

$\hat{y}_u = softmax\left(W_{cls}^{\tau(u)} h_u^{(L)}\right)$,

$U_u = -\sum_c \hat{y}_{u,c} log \hat{y}_{u,c}$

$\text{critical_score}_u = \alpha \cdot x_{physics,u} + \beta \hat{y}_{u,1} + \gamma U_u$

endfor

3. Compute loss

$\mathcal{L} = \mathcal{L}_{CE} + \lambda \mathcal{L}_{physics}$

4. Backpropagation and parameter update

$\nabla_\theta \mathcal{L} \longleftarrow \frac{\partial \mathcal{L}}{\partial \theta}$

$\theta \leftarrow \theta - \eta \nabla_\theta \mathcal{L}$

Calculate $\text{stop}_{\text{epoch}}$

n←n+1
until $\text{stop}_{\text{epoch}}$ or n = N_{epoch}
Return θ, $\hat{y}_u$, critical_score_u

4.3. Methodology to validate the trained physics-informed heterogeneous graph transformer model

The validation of the proposed physics-informed heterogeneous graph transformer (HGT) model is carried out through a multi-stage evaluation designed to assess predictive performance, generalization ability, class-wise behavior, and physical consistency of the model outputs.

The convergence and generalization ability of the model are evaluated by analyzing the dynamics of the accuracy functions over training epochs. The HGT model demonstrates stable convergence if:

$$\lim_{t\to T}\left|A_{\text{train}}^{(t)} - A_{\text{val}}^{(t)}\right| \le \epsilon_1 \tag{26}$$

Where $\epsilon_1 = 0.05$ is the acceptance criterion. This threshold is consistent with common practice in deep learning, where a gap below 5% between training and validation performance indicates good generalization and absence of overfitting [15].

The overall predictive performance of the model is quantified using classification accuracy on the test dataset:

$$Accuracy = \frac{1}{V}\sum_{v\in V} \mathbb{I}(\hat{y}_v = y_v) \ge \Theta_{accuracy} \tag{27}$$

Where Θ_{accuracy}=0.9 is the acceptance criterion. A threshold of 90% is commonly adopted in classification tasks as an indicator of reliable predictive performance [16].

The confusion matrix to be used to analyze the distribution of correct and incorrect predictions across all classes. This enables identification of systematic misclassification patterns and provides insight into class imbalance effects, which is particularly important for heterogeneous graphs with uneven node distributions.

The discriminative capacity of the classifier is evaluated using Receiver Operating Characteristic (ROC) curves and the corresponding Area Under the Curve (AUC) metric for each class. For each class c, the AUC is defined as:

$$AUC_c = \left(\int_0^1 TPR_c(FPR_c^{-1}(t))\,dt\right) \ge \Theta\text{auc} \tag{28}$$

Where Θ_{auc} = 0.8 is the acceptance criterion. This threshold follows standard classification benchmarks, where AUC $\geqslant$ 0.8 is considered good, while values above 0.9 indicate a very good discrimination [17].

To evaluate HGT model performance, class-specific metrics are computed, including Precision, Recall, and F1-score:

$$Precision_c = \frac{TP_c}{TP_c+FP_c},\ Recall_c = \frac{TP_c}{TP_c+FN_c},\ F1_c = \frac{2\cdot Precision_c\cdot Recall_c}{2\cdot Precision_c+Recall_c} > \Theta_{F1} \tag{29}$$

Where F1c = 0.8 is the acceptance criterion [18].

The alignment between model predictions and physics-based indicators is evaluated using the mean absolute physics-alignment error:

$$E_{\text{phys}}^{\text{MAE}} = \frac{1}{N}\sum_{u=1}^{N}\left|\hat{y}_{u,1} - x_{\text{physics,u}}\right| \le \theta_{E_{\text{phys}}^{\text{MAE}}} \tag{30}$$

Where $\theta_{E_{\text{phys}}^{\text{MAE}}} = 0.15$ is the acceptance criterion. The threshold is consistent with practices in physics-informed machine learning, where deviations below 10–15% are considered indicative of good physical consistency [19].

To validate that the model captures physically meaningful degradation trends the relationship between predictions and physics-based indicators is assessed using the Spearman rank correlation coefficient:

$$\rho = corr_{spearman}\left(\hat{y}_{u,1}, x_{\text{physics,u}}\right) \ge \theta_\rho \tag{31}$$

Where $\theta_\rho = 0.7$ is the acceptance criterion.

The model is considered valid if the conditions (26) - (31) are satisfied simultaneously. This ensures that the proposed approach achieves not only high predictive accuracy but also robust generalization, reliable uncertainty estimation, and consistency with underlying physical processes.

5. Experiment Preparation

The experimental setup includes construction of heterogeneous graphs from BIM models, generation of a physics-informed synthetic dataset, and configuration of the training environment.

The heterogeneous graph G= (V, E, X) used in the experiments was constructed from IFC4-based BIM models using the BuildIFCGraph method, which integrates geometric, topological, and semantic information of building structures according to methodology proposed and verified in [20]. In accordance with this approach, the graph generation process includes structural elements such as IfcBeam, IfcColumn, IfcSlab, IfcWall are mapped to node types T. Each edge is assigned to a relation type $\phi(euv) \in R$, distinguishing structural and adjacent interactions.

The HGT model was trained and evaluated on a synthetic dataset generated from IFC4 BIM models. The physical behavior of construction elements was modeled according to the methodology proposed in [9].

The dataset is split into training, validation, and test subsets. The HGT model is trained according to Algorithm 1 with the configuration: multi-head attention with H is 4; L message-passing layers is 3; maximum number of epochs Nepoch is 100; optimization using gradient descent with learning rate η is 1.2.

The models were developed and trained using the Python programming language in the following software environment: PyTorch (version 2.7.0+cpu), NumPy (version 2.2.4), Pandas (version 2.2.3), Scikit-learn (version 1.6.1), Matplotlib (version 3.10.1).

6. Experiment Results

Fig. 1. shows the dynamics of the loss and accuracy functions on the training and validation datasets over 80 epochs. Both loss curves (train loss and validation loss) steadily decrease, reaching values of approximately 0.74 and 0.61 in the final epochs. The training was stopped according to early stop criteria as validation loss curve stops improving after epoch 76. The accuracy curves (train accuracy and validation accuracy) increase synchronously and remain close to each other. In the final epoch $\left|A_{train}^{(80)} - A_{val}^{(80)}\right| = 0.001$ which is less than acceptance criterion (26). The absence of a significant gap between the training and validation curves indicates good generalization ability of the HGT model and no overfitting.

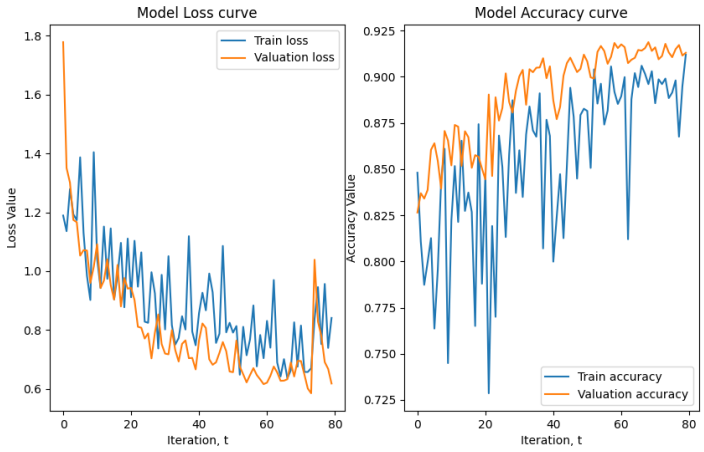


Fig. 1. Dynamics of loss and accuracy functions on the training and validation datasets of HGT model.

The overall accuracy of the model on the test dataset, which consists of 6,828 elements, is 92.06% (Fig. 2.) which satisfy acceptance criteria (27). Analysis of the ROC (Receiver Operating Characteristic) curves in Fig. 3. satisfies acceptance criteria (28) per node type. The area under the curve (AUC) confirms the model's ability to distinguish them: beam: 1.0 (suggests perfect separation of dataset); column: 0.998 (almost perfect); wall: 0.997 (almost perfect); slab: 0.845 (good quality).

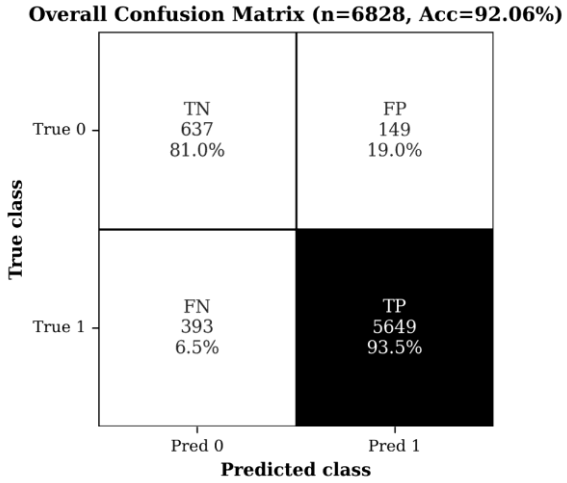


Fig. 2. Overall confusion matrix of HGT model on the test dataset.

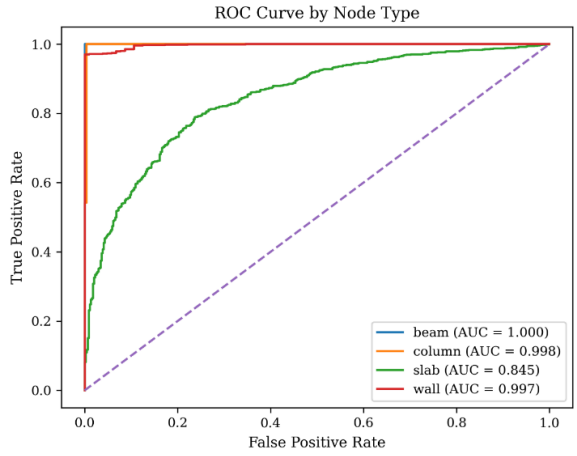


Fig. 3. ROC curves for the classes in HGT model test set.

A bar chart of the Precision, Recall, and F1-score metrics, along with confusion matrices, is presented in Fig. 4–5 and Table 1.

For the beam class, all metrics (Precision, Recall, F1-score) are equal to 1.0. The confusion matrix confirms that all 171 beams were classified correctly, with no false positives.

The model's performance for the Wall class is evaluated with an F1-score of 0.98, achieved due to nearly perfect precision (Precision ≈ 1.0) and high recall (Recall ≈ 0.97). The model's errors for this class–FN (false negatives) and FP (false positives) are 2.7% and 3.8%, respectively.

The Slab class is the most challenging for the model, with an F1-score of 0.85. The main issue is relatively low recall (Recall ≈ 0.79), as seen in the confusion matrix: 269 slabs (20.8%) were incorrectly missed (False Negatives). At the same time, precision remains high (≈ 0.88), meaning that elements classified as slabs are mostly correct.

For the Column class, the model achieved perfect recall (Recall = 1.0), meaning it successfully found all 24 columns in the test set. However, this was at the cost of low precision (Precision ≈ 0.39), as the model incorrectly classified 37 other elements as columns (False Positives).

F1-score satisfies acceptance criteria (29) for all nodes except for rare class 'column'. Given the safety-critical nature of inspection tasks and the achieved perfect recall (Recall = 1.0), this deviation is considered acceptable.

Table 1. Classification metrics for the classes in HGT model test set.

Node Type	Accuracy	Precision	Recall	F_1	n	TP	TN	FP	FN
beam	1	1	1	1	180	171	9	0	0
column	0.86	0.39	1	0.56	258	24	197	37	0
slab	0.78	0.9	0.79	0.84	1734	1026	331	108	269
wall	0.97	0.99	0.97	0.98	4656	4428	100	4	124

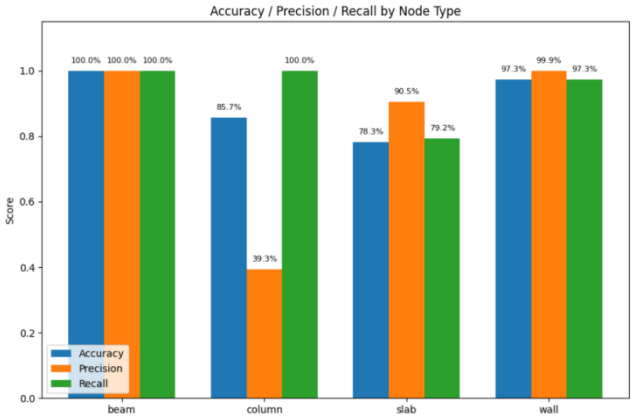


Fig. 4. Bar chart of Precision, Recall, and F1-score metrics for the classes in HGT model test set.

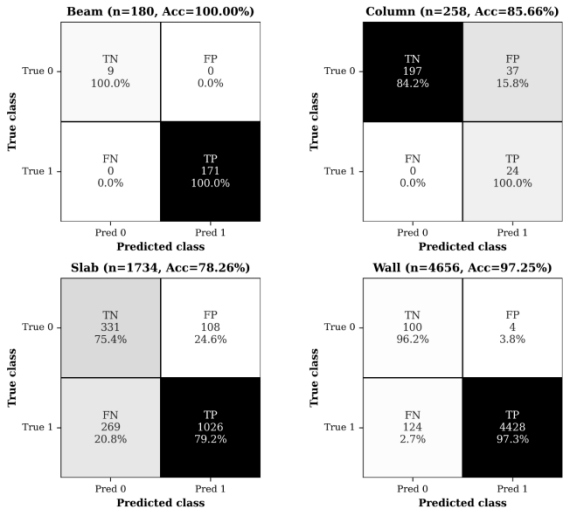


Fig. 5. Confusion matrices for the classes in the model test set.

Dynamics of predicted probabilities and physics-based indicators are illustrated on Fig. 6 and corresponding metrics are included in Table 2. The alignment between model predictions and physics-based indicators measured by $E_{\text{phys}}^{\text{MAE}} = 0.027 \leq 0.15$ which satisfies criteria (30). The validation that the model captures physically meaningful degradation trends measured by Spearman rank correlation coefficient = 0.855 is above 0.7 which satisfies criteria (31).

Visualization of the dynamics of the criticality score of the nodes defined in section 4.2, using the heterogeneous graph of AC20-FZK-Haus.ifc is shown in Fig. 7.

The model's attention, expressed through the critical score metric: At the initial stage (t=2, number of days = 60), HGT model's attention is mainly based on the input features of the node itself, with minimal influence from neighbors. 18 out of 21 elements are marked in green, meaning their condition does not require inspection (Fig. 7 (a)). At stage (t=15), time-dependent degradation caused the term $x_{physics,u}$ of the critical score formula increased for all elements, which was confirmed by the model's probability as a result, 18 elements are marked in yellow, meaning their condition needs to be inspected (Fig. 7 (b)).

A critical score greater than 0.8 for two slab-type elements at steps t=2 and t=15 is consistent with the quantitative metrics presented earlier in Fig. 4. The slab class demonstrated the lowest recall (Recall = 0.79), indicating the model's difficulty in identifying these elements, and thus a high value of the "uncertainty" component in critical score formula causes nodes of slab class are red.

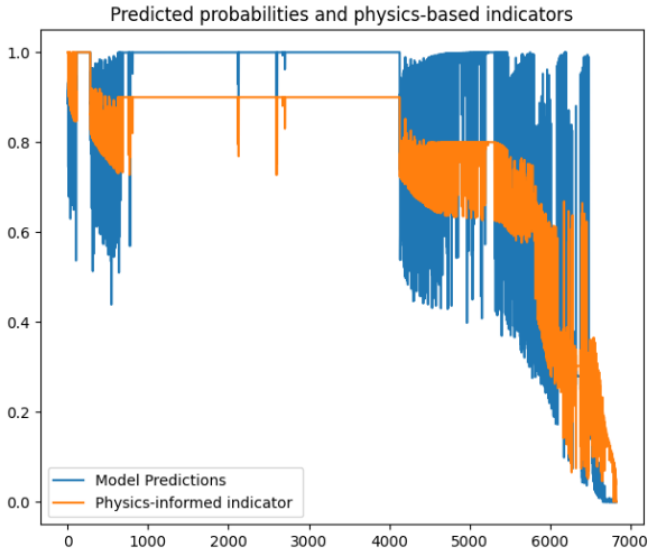


Fig.6. Dynamics of predicted probabilities and physics-based indicators

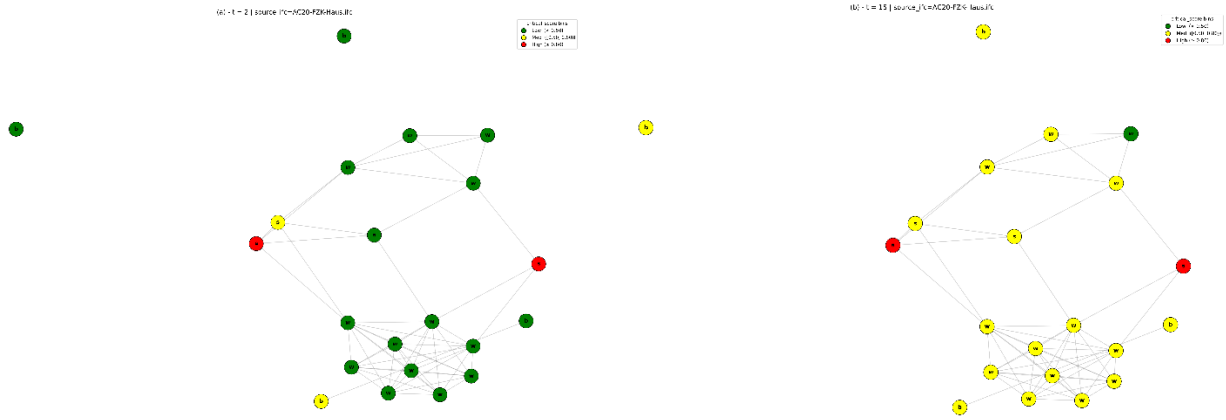


Fig.7. Dynamics of the criticality score of nodes on heterogeneous graph of AC20-FZK-Haus.ifc: (a) – nodes' critical score at initial stage t=2; (b) - nodes' critical score at stage t=15.

In summary, the acceptance criteria defined in section 4.3 are achieved in the results so the proposed physics-informed HGT model provides predictive performance, also interpretable and physically consistent assessment of structural elements, enabling identification and prioritization of components requiring inspection.

7. Discussions

The achieved overall accuracy of 92.06% on our synthetic dataset demonstrates improvement over methods in the reviewed papers, which reported accuracy of approximately 85%-89% on a similar element classification task (Table 2). This highlights the benefit of integrating physics-informed features for enhancing predictive reliability. The strong AUC scores across all classes (Fig. 3), particularly for 'beam' (1.0), 'column' (0.998), and 'wall' (0.997), further underscore the model's discriminative capability.

Table 2. Achieved overall accuracy comparison results

Method / Reference	Model Type	Data Source	Physics Integration	Accuracy
BIM-HGNN [3]	Heterogeneous GNN	BIM (IFC)	None	~0.85
BIGNet [4]	Pretrained HGNN	BIM (static)	None	~0.88
ContextNet [6]	Dual-encoder GNN	BIM geometry	None	~0.86
Transformer BIM-IoT [7]	Transformer	BIM + IoT	None	~0.89
Proposed HGT	Physics-informed Heterogeneous Graph Transformer	BIM (IFC) + synthetic physics data	Explicit	0.9206

A limitation of this study is its reliance on a synthetic dataset. While this allowed for controlled validation, future work must focus on applying and validating the proposed model on real-world data from active construction projects to further assess its robustness and practical applicability. An additional limitation is the low precision observed for the 'column' class, which points to a challenge with severe class imbalance. Future research could explore advanced sampling strategies or modified loss functions to improve this metric without sacrificing the essential high recall.

8. Conclusion

This study proposed a physics-informed heterogeneous graph transformer model as a core component of a hybrid information technology for managing heterogeneous big data in urban construction projects, enabling prediction of the technical condition and inspection needs of structural elements. The developed model incorporates structural domain knowledge through physics-informed features and a dedicated regularization term in the loss function, enabling both data-driven learning and physical consistency of predictions.

The validation of the proposed model was carried out according to the multi-criteria framework defined in Section 4.3, covering convergence, predictive performance, discriminative ability, class-wise behavior, and physics consistency. The results obtained confirm that all key validation criteria are satisfied under the conducted experimental conditions:

The convergence criterion (26) is fulfilled, as the difference between training and validation accuracy remains within the threshold ($\epsilon_1 = 0.05$), indicating stable learning and absence of overfitting.

The overall classification accuracy exceeds the required threshold ($\theta_{accuracy} = 0.9$), reaching 92.06%, demonstrating strong predictive capability.

The discriminative performance meets criterion (28), with AUC values above 0.8 for all classes, including a good separation for beam, column, and wall elements.

The class-wise performance satisfies criterion (29) for all major classes, with a deviation for the rare “column” class. This deviation is acceptable due to the safety-critical requirement of maximizing recall, which was achieved at 1.0.

The physics consistency criteria (30) – (31) are satisfied, with low physics-alignment error ($E_{phys}^{MAE} = 0.027 \leq 0.15$) and strong spearman correlation with physics-based indicators ($\rho = 0.855 \geq 0.7$), confirming that the model captures meaningful degradation processes.

Thus, the validation criteria (26) – (31) are simultaneously satisfied, which verifies the correctness, robustness, and applicability of the proposed approach.

The proposed model novelty is a developed physics-informed graph learning paradigm for construction systems.

The practical significance of the proposed approach is its ability to support predictive maintenance and inspection planning; early detection of structural and functional anomalies; optimization of resource allocation in urban construction projects; enhanced safety and sustainability of built environments.

Future work focus will be integration of the designed physics-informed heterogeneous graph transformer model in the hybrid information technology framework for managing heterogeneous Big Data in urban construction projects.

All the Declarations and Statements

Author Contribution Statement

O. Solovei – Design of the architecture of physics-informed heterogeneous graph transformer model; design of methodology to train a physics-informed heterogeneous graph transformer model; design of methodology to validate the trained physics-informed heterogeneous graph transformer model.
T. Honcharenko – Conceptualization, Supervision: Proposed research ideas.

All authors have read and agreed to the published version of the manuscript.

Conflict of Interest Statement

The Authors declared no conflicts of interest**.**

Funding Declaration

This research received no external funding.

Data Availability Statement

The data that support the findings of this study are from the corresponding author upon reasonable request.

Ethical Declarations

This study did not involve human participants or animals**.**

Acknowledgements

None.

Declaration of Generative AI in Scholarly Writing

During the preparation of the manuscript, the authors carefully reviewed the content and take full responsibility for the accuracy and integrity of the manuscript.

Abbreviations

The following abbreviations are used in this manuscript:

IFC - Industry Foundation Classes.
BIM - Building Information Modeling.
HGT - heterogeneous graph transformer.
AUC - Area Under the Curve.

Appendix A\B\C…, with appendix tile

None.

References

[1] D. Kumar, K. K. Maurya, S. K. Mandal, B. A. Mir, A. Nurdiawati, and S. G. Al-Ghamdi, "Life cycle assessment in the early design phase of buildings: Strategies, tools, and future directions," Buildings, vol. 15, no. 10, p. 1612, 2025. doi:10.3390/buildings15101612.

[2] Y. Zhang et al., "MetaCity: Data-driven sustainable development of complex cities," The Innovation, vol. 6, no. 2, 2025. doi:10.1016/j.xinn.2024.100775.

[3] W. Zhang, Z. Wang, Z. Yang, and Z. Cai, "BIM-based spatial semantic reasoning and lifecycle management driven by heterogeneous graph neural networks," SSRN, 2024. Available: https://papers.ssrn.com/sol3/papers.cfm?abstract_id=5678364 (accessed Mar. 28, 2026).

[4] J. Han, X. Z. Lu, and J. R. Lin, "Pretrained graph neural network for embedding semantic, spatial, and topological data in building information models," Computer-Aided Civil and Infrastructure Engineering, vol. 40, no. 26, pp. 4607–4631, 2025. doi:10.1111/mice.70073.

[5] G. Austern, T. Bloch, and Y. Abulafia, "Incorporating context into BIM-derived data–leveraging graph neural networks for building element classification," Buildings, vol. 14, no. 2, p. 527, 2024. doi:10.3390/buildings14020527.

[6] N. Kayhani, B. McCabe, and B. Sankaran, "BIM-based construction quality assessment using graph neural networks," in Proc. Int. Symp. Automation and Robotics in Construction (ISARC), vol. 40, pp. 9–16, 2023.

[7] H. Yu, T. Hou, and Y. Lin, "Enhancing graph transformer encoding with graph heterogeneous memory for improved recommendation performance," Scientific Reports, vol. 15, no. 1, p. 44567, 2025. doi:10.1038/s41598-025-28266-1.

[8] C. Meng and S. Wang, "Transformer-based energy consumption prediction and optimization framework for BIM-enabled green buildings," in Int. Conf. Computer Vision and Machine Learning (CVML 2025), vol. 14065, pp. 12–20, SPIE, Feb. 2026. doi:10.1117/12.3100406.

[9] O. Solovei, "Physical state models of structural elements for predicting building reliability using graph neural networks," Herald of Khmelnytskyi National University. Technical Sciences, vol. 363, no. 2, pp. 563–575, 2026. doi:10.31891/2307-5732-2026-363-75.

[10] G. H. Nayak et al., "Transformer-based deep learning architecture for time series forecasting," Software Impacts, vol. 22, p. 100716, 2024. doi:10.1016/j.simpa.2024.100716.

[11] A. Rogers, O. Kovaleva, and A. Rumshisky, "A primer on neural network architectures for natural language processing," Journal of Artificial Intelligence Research, vol. 69, pp. 1–16, 2020.

[12] S. Khan et al., "Transformers in vision: A survey," ACM Comput. Surv., vol. 54, no. 10s, pp. 1–41, 2022. doi:10.1145/3505244.

[13] C. Chen et al., "Uncertainty quantification on graph learning: A survey," arXiv preprint arXiv:2404.14642, 2024.

[14] J. Von Oswald et al., "Transformers learn in-context by gradient descent," in Int. Conf. Machine Learning, PMLR, pp. 35151–35174, July 2023.

[15] L. Prechelt, "Early stopping-but when?," in Neural Networks: Tricks of the Trade, Berlin, Heidelberg: Springer, 2002, pp. 55–69.

[16] G. Nicora, M. Rios, A. Abu-Hanna, and R. Bellazzi, "Evaluating pointwise reliability of machine learning prediction," Journal of Biomedical Informatics, vol. 127, p. 103996, 2022. doi:10.1016/j.jbi.2022.103996.

[17] S. Sathyanarayanan and B. R. Tantri, "Confusion matrix-based performance evaluation metrics," African Journal of Biomedical Research, vol. 27, no. 4S, pp. 4023–4031, 2024. doi:10.53555/AJBR.v27i4S.4345.

[18] D. Chicco and G. Jurman, "The Matthews correlation coefficient (MCC) should replace the ROC AUC as the standard metric for assessing binary classification," BioData Mining, vol. 16, no. 1, p. 4, 2023. doi:10.1186/s13040-023-00322-4.

[19] M. Raissi, P. Perdikaris, and G. E. Karniadakis, "Physics-informed neural networks: A deep learning framework for solving forward and inverse problems involving nonlinear partial differential equations," Journal of Computational Physics, vol. 378, pp. 686–707, 2019.

[20] O. Solovei and T. Honcharenko, "Method for creating graphs based on BIM models for predictive monitoring of buildings," Management of Development of Complex Systems, no. 64, pp. 247–258, 2025. doi:10.32347/2412-9933.2025.64.247-258.

Authors' Profiles



Dr. Olga Solovei received her PhD in computer science from Kyiv National University of Construction and Architecture, Kyiv, Ukraine, in 2013. Her research focuses on the development of models and methods for Big Data science theory. She is currently an Assistant Professor of the Department of Information Technologies and Doctoral Student of the Department of Information Technologies, Kyiv National University of Construction and Architecture, Kyiv, Ukraine.



Dr. Tetyana Honcharenko is Doctor of Technical Sciences and Professor in Computer Science from Kyiv National University of Civil Engineering and Architecture. Her research focuses on the development of models and methods for Big Data science theory, Information technologies and Digital Twins in construction, BIM and Artificial Intelligence. In the Scopus she has 41 scientific publications, and her h-index is 13 (ID 57204204504). She is a full member of the Academy of civil engineering of Ukraine since 2021. She is a member of the subcommittee F3 Computer Science of the higher education sector of the scientific and methodological council of the Ministry of Science and Education of Ukraine since 2024. She is currently Head of the Department of Information Technologies, Kyiv National University of Civil Engineering and Architecture, Kyiv, Ukraine. She is the Head of the scientific project "Methodology of determining tonality and classification of multimodal content in territorial revitalization projects based on neural network methods".

How to cite this paper

Olga Solovei, Tetiana Honcharenko, "A Physics-Informed Heterogeneous Graph Transformer Model for Managing Heterogeneous Big Data in Urban Construction Projects", International Journal of Wireless and Microwave Technologies(IJWMT), Vol.16, No.3, pp. 128-141, 2026. DOI:10.5815/ijwmt.2026.03.09